J. Am. Chem. Soc. 1986, 108, 1521-1531

A Surface Force Field Model for the Molecular Mechanics Simulation of Ligand Structures in Transition-Metal Carbonyl Clusters

Joseph W. Lauher

Contribution from the Department of Chemistry, State University of New York, Stony Brook, New York 11794. *Received August 1, 1985*

Abstract: A surface force field is developed for the molecular mechanics simulation of ligand structures in transition-metal carbonyl clusters. A smooth continuous surface for a metal cluster is defined as the border of the region of space that cannot be penetrated by a probe sphere. The surface represents the bottom of the potential well corresponding to the bond stretch between the carbon atom of a carbonyl ligand and the metal cluster. The distance parameters used to define the cluster surface are chosen such that the M–C distances will correspond to experimental values for all types of carbonyl ligands: terminal, semibridging, and symmetrical bridging. Additional terms are added to the force field representing the C–O stretch, the M–C–O bend, and the nonbonded van der Waals and electrostatic interactions. Minimized structures were calculated for a variety of transition-metal clusters. A steric energy is assigned to each, defined as the total energy divided by the number of carbonyl ligands in the cluster. The clusters with the highest steric energies have the most crowded ligand structures and include $Fe_2(CO)_9$, $Fe_3(CO)_{12}$, and $CrFe_3(CO)_{14}^{2-}$. Of the clusters studied those with the lowest steric energies are the $M_4(CO)_{12}$ clusters. The lowest energy geometry for a $M_4(CO)_{12}$ cluster is an all terminal structure with *T* point group symmetry. The structure has never been seen in any derivative of a $M_4(CO)_{12}$ cluster but does serve as the basis for the structures of the clusters $Fe_4(CO)_{13}^{2-}$ and $CoFe_3(CO)_{13}^{-}$.

The bonding capabilities of transition-metal clusters are reasonably well understood.[1] The correlations between metal core geometries and the stochiometries of ligand bonding are well established and are nicely summarized by standard empirical rules.[2,3] Thus for a particular transition-metal cluster, M_x^{n-}, made up of a given number of metal atoms in a fixed geometry with a defined charge, the number of ligands, carbon monoxide, for example, required for the formation of a stable molecular species, $M_x(CO)_y^{n-}$, can easily be determined. Not so simple is the problem of ligand structure, the arrangement of the ligands in space upon the surface of the metal core.

Consider the case of a M_2 cluster with 8 carbonyl ligands, $M_2(CO)_8^{n-}$. There are three well-characterized examples: $Co_2(CO)_8$, $FeCo(CO)_8^-$, and $Fe_2(CO)_8^{2-}$. They form an isoelectronic series with 34 cluster valence electrons (CVEs), but the ligand structures are very different. In the solid state[4] $Co_2(CO)_8$ has a C_{2v} structure with two bridging carbonyl ligands, $Fe_2(CO)_8^{2-}$ has a D_{3d} structure with no bridging carbonyl ligands,[5] and $FeCo(CO)_8^-$ has a more complex C_s structure with one "semibridging" carbonyl ligand.[5] In solution the $Co_2(CO)_8$ molecule adopts the D_{3d} structure with a minor isomer that most likely has a D_{2d} geometry.[6-9] The anion $Fe_2(CO)_8^{2-}$ also exists as a mixture of isomers in solution.[8] Similar variations in ligand structure are typical in most other binary metal carbonyl systems and can be extremely complex in some cases.

Solution dynamics indicate that the carbonyl ligands are often mobile and able to move readily about the surface of a cluster. A given carbonyl can bond to a cluster in a variety of ways. It can bond in a terminal mode to one metal atom or in a bridging mode to two or three metal atoms. The bridges can be symmetrical with equal distances to each of the involved metal atoms or they can be asymmetric with differing distances. Extreme asymmetry evolves into terminal bonding; intermediate cases are often termed "semibridging". The net energy of metal carbonyl bonding appears to be similar for each of the various modes of bonding. This is known from direct thermodynamic measurements in a few cases and can be in inferred from the easy interconvertibility of various isomers of a given molecule.

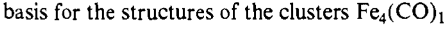

The question of ligand structure in cluster compounds was first discussed by Dahl and his co-workers in their classic papers on the structure analyses of some of the most important binary carbonyls. They noted[10] that the CO ligands in a binary carbonyl, such as $Fe_3(CO)_{12}$, adopt a structure such that the oxygen atoms of the carbonyl ligands approximately define the vertices of a symmetrical polyhedron, the icosahedron in the case of $Fe_3(CO)_{12}$. They suggested that this wide-spread effect was presumably due to a favorable packing of the CO ligands about the cluster core.

Johnson investigated these ideas systematically for a wide variety of binary metal carbonyls.[11-13] In his investigations he considered a CO_y collection of carbonyl ligands arranged in space in the form of the polyhedron most favored by packing forces. The metal polyhedron, M_x, was then considered to position itself within the CO polyhedron in an orientation that maximized bonding between the metal atoms and the carbonyls in the resulting $M_x(CO)_y$ cluster compound. In the Johnson model the relative sizes of the CO polyhedron vs. the metal polyhedron are very important considerations and can be used to explain the differences between ligand structures in an isoelectronic series. Thus $Fe_3(CO)_{12}$ has the favored icosohedral packing of CO ligands, while the CO ligands of $Os_3(CO)_{12}$ adopt the less effective packing of an anticubeoctahedron in order to accommodate the larger Os_3 core.[11]

In later work Johnson developed a more quantitative analysis and presented a systematic study of ligand structures with up to 16 carbonyls. This was done by using a simple points on a sphere repulsion model used earlier for the determination of ligand

---

(1) Lauher, J. W. *J. Am. Chem. Soc.* **1978**, *100*, 5305; **1979**, *101*, 2604. Lauher, J. W. *J. Organomet. Chem.* **1981**, *213*, 25.

(2) Mingos, D. M. P. *Nature* **1972**, *236*, 99.

(3) Wade, K. *Chem. Britain* **1975**, *11*, 177. Wade, K. *Adv. Inorg. Chem. Radiochem.* **1976**, *18*, 1.

(4) Sumner, G. G.; Klug, H. P.; Alexander, L. E. *Acta Crystallogr.* **1964**, *17*, 732.

(5) Chin, H. B.; Smith, M. B.; Wilson, R. D.; Bau, R. *J. Am. Chem. Soc.* **1974**, *96*, 5285.

(6) Bor, G.; Dietler, U. K.; Noack, K. *J. Chem. Soc., Chem. Commun.* **1976**, 914.

(7) Sweany, R. L.; Brown, T. L. *Inorg. Chem.* **1977**, *16*, 415.

(8) Onaka, S.; Shriver, D. F. *Inorg. Chem.* **1976**, *15*, 915.

(9) Lichtenberger, D. L.; Brown, T. L. *Inorg. Chem.* **1978**, *17*, 1381.

(10) Wei, C. H.; Dahl, L. F. *J. Am. Chem. Soc.* **1969**, *91*, 1351.

(11) Johnson, B. F. G. *J. Chem. Soc., Chem. Commun.* **1976**, 211.

(12) Johnson, B. F. G.; Benfield, R. E. *J. Chem. Soc., Dalton Trans.* **1978**, 1554.

(13) Benfield, R. E.; Johnson, B. F. G. *J. Chem. Soc., Dalton Trans.* **1980**, 1743.

0002-7863/86/1508-1521$01.50/0

structure in single metal systems.[12,13] The Johnson model can rationalize the gross ligand structure in most binary carbonyl systems, but it is not capable of providing detail.

For detail, molecular orbital methods can be used, but realistically the complexity of the problem, with a lower energy surface connecting many structures in a multimetallic system, is beyond the capabilities of present day molecular orbital methods. A new approach is needed for the meaningful calculations of ligand structures.

The complexity of the ligand structure problem is actually much more difficult than presented here so far. The binary carbonyl systems represent the simplest case. When other ligands such as π-bonded hydrocarbons or phosphines are considered the problem becomes much more difficult. Mixed metal clusters that contain more than one type of metal atom would also present greater difficulties.

The Molecular Mechanics Approach. For organic molecules, structures and thermodynamic properties can be determined by a force field or molecular mechanics approach.[14] In the calculations a connectivity is assumed for a molecule and forces are assigned to bond stretches and bends, dihedral angles, and nonbonded interactions. Special account is given to special problems such as hydrogen bonds, lone pairs, and bond polarities and a minimization in coordinates with respect to the assigned forces is performed. The method has been extremely successful and is widely used. A similar approach has been developed for conformational studies of proteins and other macromolecular systems of biochemical interest.

Applications of molecular mechanics have also been made in inorganic systems and have been particularly successful in analyses of conformations in metal chelate systems.[15] Applications to systems with metal–metal bonds have only just begun and have consisted of extensions of the force fields developed for organic systems.[16-18] Horwitz, Holt, and Shriver have developed a simple force field model for analyzing one particular sterically crowded metal carbonyl compound.[19]

It should be possible to use a molecular mechanics approach for a comprehensive study of the ligand structure problem. However, the methods developed for organic systems cannot be simply adopted for the problem, because two of the fundamental assumptions of molecular mechanics break down when applied to cluster compounds.

Perhaps the first assumption in any force field or molecular mechanics calculation is one of atom connectivity. The atoms bonded to one another are defined and are assigned force constants associated with the given bond type. Other types of forces are assumed between nonbonded atoms. It is difficult to assign connectivity in cluster systems. Even with the results of an X-ray crystal structure determination to examine, organometallic chemists would not always agree upon the assignments of atom connectivity in a given transition-metal cluster compound. As discussed in the introduction a carbonyl ligand can bind to a cluster in many ways with a smooth variation from the terminal mode, to semibridging, to asymmetric bridging, to symmetric bridging. With such a variable system no atom by atom assignment of bonds and associated force constants can possibly be meaningful. More meaningful is a simple assumption that the CO ligands are bonded not to a single metal atom but to the metal core of the compound as a whole.

A second assumption of standard molecular mechanics methods that does not readily extend to cluster systems is the definability of geometry about a central atom. In a standard molecular mechanics calculation any given atom is assumed to have a certain connectivity and an associated preferred geometry. Thus the angle force constants associated with a four-coordinate carbon atom are assigned a minimum corresponding to the tetrahedral angle. In most organometallic systems the angles between the ligands about a central atom show too much variation for the intelligent assignment of meaningful bond angle force constants. This is not a major problem, however, because the extreme variability of angles suggests that the energy surface is very flat and that direct nonbonded forces between the ligands may indeed dominate over any metal-centered angular term.

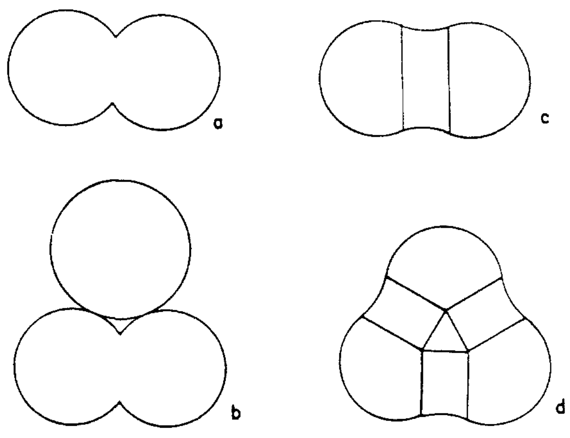

Figure 1. (a) The union of two spheres of radius r_t at a distance of $2r_m$ apart. (b) A probe sphere of radius r_p in contact with the union of two spheres. (c) The cluster surface, defined as the border of the region of space that cannot be penetrated by the probe sphere. The diameter of the probe sphere, r_p, is chosen such that the innermost contact point is at a distance r_b from the metal centers. There are two types of regions to this cluster, two convex regions and a central saddle region. (d) A cluster surface for a trinuclear cluster. There are three types of regions for this cluster, convex regions corresponding to the terminal carbonyl region, saddle regions corresponding to bridging carbonyl region, and the central concave region corresponding to the triple bridging carbonyl region.

In this paper I would like to report the development of a new surface force field model that avoids these difficulties and allows a meaningful molecular mechanics treatment of transition-metal carbonyl clusters.

An Equal Potential Surface for a Cluster. The preferred bonding of a carbonyl ligand to a single metal atom can be modeled in part by defining a sphere about the metal atom with a radius equal to the minimum of the potential well corresponding to the bond between the metal atom and the carbon atom of the carbonyl ligand; 1.75 Å might be a reasonable value. In this model a single carbonyl would be free to move about the surface of the sphere with no change in energy, but movements perpendicular to the surface of the sphere would require the expenditure of energy. If two metal atoms form a dimer with a typical metal–metal bond distance of 2.6 Å, the spheres of equal potential around each metal atom would intersect (Figure 1a). A new surface defined by the union of the two spheres could be used to represent the equal potential surface of the two-metal cluster, but there would be serious problems associated with the cusp at their juncture. The cusp can be removed and the surface improved by a smoothing operation using a probe sphere.

The probe sphere is conceptually allowed to roll around the surface of the union of the spheres of the metal cluster. The cluster surface is defined as the border of the region of space that cannot be penetrated by the probe sphere. In the case of a dimer the probe sphere would smooth out the cusp at the juncture of the two metal atom spheres. As the probe rolled about the dimer it would trace out a torus or doughnut-shaped figure (Figure 1b). The innermost part of the surface of the torus would become the outer surface of the cluster in the region between the metal nuclei (Figure 1c).

The radius of the probe sphere is chosen precisely such that the innermost points of the torus surface are at a distance from each metal atom equal to the minimum in the potential well

---

(14) Burkert, U.; Allinger, N. L. "Molecular Mechanics"; American Chemical Society: Washington, 1982.

(15) Brubaker, G. R.; Johnson, D. W. *Coord. Chem. Rev.* **1984**, *53*, 1.

(16) Newsam, J. M.; Halvert, T. R. *Inorg. Chem.* **1985**, *24*, 491.

(17) Newsam, J. M.; Bradley, J. S. *J. Chem. Soc., Chem. Commun.* **1985**, 759.

(18) Boeyens, J. C.; Cotton, F. A.; Han, S. *Inorg. Chem.* **1985**, *24*, 1750.

(19) Horwitz, C. P.; Holt, E. M.; Shriver, D. F. *Inorg. Chem.* **1975**, *23*, 2491.

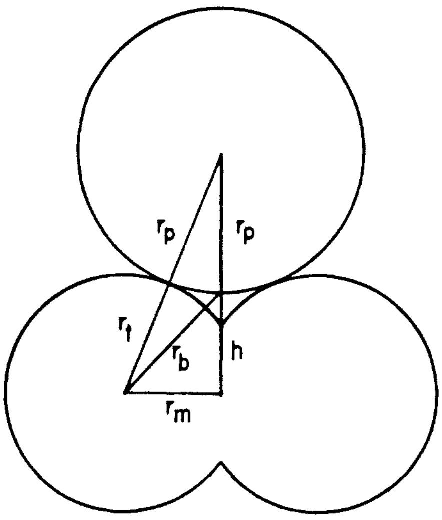

Figure 2. Sketch for the derivation of the parameters in Schemes I-III. r_t is the distance from a metal atom to the minimum of the potential well for the bond to a terminal carbonyl, r_b is the distance from a metal atom to the minimum of the potential well for the bond to a symmetrical bridging carbonyl, r_m is half the representative metal-metal bond distance. Not shown are $(4/3)^{1/2}r_m$, the distance from a metal atom to the center of an equalateral triangle of metal atoms, h_c, the distance from the center of the triangle to the bottom of a concave postion, and r_c the distance from a metal atom to the bottom of a concave position.

Scheme I

$$h = (r_b^2 - r_m^2)^{1/2}$$

$$(r_p + r_t)^2 = (r_p + h)^2 + r_m^2$$

$$r_p = \frac{h^2 + r_m^2 - r_t^2}{2(r_t - h)}$$

representing the bond from the carbon atom of a symmetrical bridging carbonyl ligand to a metal atom.

This same procedure can be used for a cluster of any size with any number of metal atoms. In a triangle of metal atoms the probe sphere could not trace out an entire torus about the metal-metal bond of two of the metal atoms, because at two points, one above and one below the surface of the cluster, the probe sphere would encounter the third metal atom. At these two points the probe sphere would be tangent simultaneously with all three spheres and would define a concave section of the cluster surface (Figure 1d).

The entire surface of any metal cluster will have three types of regions, convex regions defined by the exposed surfaces of the original metal atom spheres, saddle-shaped regions defined as the inner portion of a torous traced by a probe sphere moving about a metal-metal bond, and concave regions defined by the probe sphere resting tangent to three or more spheres.

This representation of a cluster surface is identical in construction with that developed by Conolly for the computation of molecular volumes of proteins.[20] Connolly gave a definition for the molecular volume of a protein as that part of space not accessible by a hard sphere representing a solvent molecule. More precisely he defined the term "solvent-accessible surface ... used to refer to the smooth network of convex and reentrant surface traced by the inward-facing part of the probe sphere as it rolls over the molecule."[20] In his paper Connolly has a series of color figures that nicely illustrate the solvent-accessible surfaces. The reader of this paper may wish to examine his figures to better understand the surfaces derived here for metal clusters. In particular the three different surface regions, convex, saddle, and concave, are clearly illustrated.

The analytical solution for the calculation of the solvent-accessible surface is given by Connolly as a set of equations. The calculation of the equal potential surface for a metal cluster as discussed above can be calculated by using the same equations. The only input needed is the coordinates of the metal atoms, the radius, r_t, of the metal spheres defined as the distance from a metal atom to the bottom of the potential well of a terminal carbonyl ligand, and the radius, r_p, of the probe sphere (Figure 2). The value for r_p is calculated by using the equations of Scheme I. The value depends upon r_m, defined as half the bond length of a chosen representative metal-metal bond within the cluster, and r_b, the distance from a metal to the bottom of the potential well corresponding to a symmetrical bridging carbonyl ligand. This means that as a carbonyl moves about the equal potential surface it will be at the proper terminal distance when it is near one metal and will be at the proper bridging distance when it is near more than one metal with a smooth transition in between.

Scheme II

$$(r_p + r_t)^2 - r'^2_m = (r_p + h')^2$$

$$h' = ((r_p + r_t)^2 - r'^2_m)^{1/2} - r_p$$

$$r'_b = (h'^2 + r'^2_m)^{1/2}$$

Scheme III

$$(r_p + r_t)^2 - (4/3)r'^2_m = (r_p + h_c)^2$$

$$h_c = ((r_p + r_t)^2 - (4/3)r'^2_m)^{1/2} - r_p$$

$$r_c = (h_c^2 + (4/3)r'^2_m)^{1/2}$$

Table I. Calculated Double, r'_b, and Triple Bridging, r_c, Carbonyl Minima for Various Metal-Metal Distances (Å)[a]

M-M ($2r'_m$)	r'_b	r_c
2.4	1.964	2.037
2.5	1.981	2.056
2.6	(2.0)	2.080
2.7	2.019	2.105
2.8	2.038	2.130
2.9	2.059	2.157
3.0	2.080	2.184

[a] The values in the table are calculated with use of Schemes I-III with the values r_m = 1.3 Å, r_t = 1.75 Å, r_b = 2.0 Å.

Once a value for r_p is calculated it is used to define the entire cluster surface even though the metal-metal distances, r'_m, may differ from the representative value chosen for the calculation of r_p. This means that the actual bridging distance values, r'_b, will also differ. The relationship is derived in Scheme II and typical results are shown in Table I. Also of interest is the distance, r_c, to the bottom of a concave hole defined by three atoms. This distance would represent the favored position of a triple-bridging CO ligand and can be calculated with use of Scheme III. The calculated values, Table I, are just slightly longer that the r'_b values and are reasonable distances for a triple-bridging carbonyl.

This outlined model for a metal cluster may seem complicated, but the equal potential surface can easily be calculated by a computer subroutine based upon Connolly's equations. It is a general procedure that can be applied to all clusters with any number of metal atoms in all possible geometries.

The Force Field. There are many different empirical force fields available in the literature and it is difficult to choose between them. For organic molecules, Allinger's MM2 force field is probably the most widely used and is the one chosen for adaption to this study.[14,21] In the near future I plan to extent the model to hydrocarbon ligands, so it is important to adopt a force field that is already well parameterized for such compounds.

The standard MM2 approach has been modified to accommodate the surface force field discussed above. Simple bond stretches are not considered between the carbonyl carbons and the metal atoms, they are considered to be between the carbonyl carbons and the cluster as a whole. The surface as defined by the probe sphere represents the minimum of the potential well

---

(20) Connoly, M. L. *J. Am. Chem. Soc.* **1985**, *107*, 1118.

(21) Allinger, N. L. *J. Am. Chem. Soc.* **1977**, *99*, 8127.

for carbonyl bonding. The perpendicular displacement of the carbonyl carbon atom from the surface is the analogue of a conventional bond stretch. For the convex or terminal carbonyl regions of the surface the standard equation for the bond stretch, E_s, can be used for the cluster-to-carbon bond. (r is the C–M bond distance, and r_t is the standard value for the M–C bond as discussed above.)

$$E_s = 71.94K_s(r - r_t)^2(1 - 2.00\ (r - r_t)) \qquad (1)$$

For the saddle and concave or bridging regions of the surface a modified equation is used. (r' is the carbon to probe sphere center distance, and r_p is the radius of the probe sphere as discussed above.)

$$E_s = 71.94K_s(r' - r_p)^2(1 + 2.00(r' - r_p)) \qquad (2)$$

The sign of the cubic term in the equation is reversed, because the distance, r', is measured from the center of the probe sphere on the outside of the cluster. A carbon atom with a larger value of r' would be farther from the probe sphere center and thus closer to the metal atoms. Used together these two equations yield a continuous, equal potential surface for the cluster. The minimum of the potential well is smooth with no discontinuities. The important variable distance is the perpendicular distance of the carbonyl carbon atom from the surface at any given point. In the bridging carbonyl region the minimum potential will yield a continuous range of M–C bond distances corresponding to the values found for terminal, semibridging, and bridging carbonyls. As the energy minimization proceeds a given carbonyl is free to move from one region, convex, saddle, or concave, to another. The proper equation for the bond stretch is chosen automatically, depending upon the location of the carbonyl on the cluster surface.

The M–C–O bond angle calculation is also modified for similar reasons. The standard MM2 equation is used, but the angle is defined as the angle

$$E_0 = 0.021914K(\theta - \theta_0)^2(1 + 7.0(10^{-8})(\theta - \theta_0)^4) \qquad (3)$$

θ between the C–O vector and the normal to cluster surface. The minimum θ_0 is equal to 0°. For a carbonyl on the convex part of the surface this corresponds to a conventional 180° M–C–O bond angle, but for a carbonyl on saddle or concave bridging regions the conventional M–C–O bond angle will be less that 180° and will depend upon the relative values specified for r_t, r_b, and r_m.

The C–M–C angle bends are not assigned a force at all, they are completely neglected. The resulting C–M–C angles are governed entirely by the van der Waals and electrostatic interactions between the nonbonded atoms. This neglect of a specific C–M–C bending force is an important part of the model.

The C–O stretch is treated as a conventional bond stretch. The van der Waals interactions are treated by using the Allinger variant[21] of the Buckingham equation, and the electrostatic forces are calculated by using the simple coulomb potential. In the calculations reported here the metal–metal framework of the cluster was fixed, but there is nothing in the model that prevents the assignment of a suitable force constant for a metal–metal stretch. This will be an important variable in future investigations.

The actual parameters selected for the calculations reported in this paper are listed in Table II. The stretching and bonding force constants were chosen rather arbitrarily but seem to result in a reasonable range of calculated values. They are not chosen to represent any particular transition-metal element. The values for r_t, r_b, and r_m must also be specified. These distances will vary for different metals and can in principle be reset for each specific problem. In this paper two sets of values for r_t, r_b, and r_m have been chosen, one set is for first-row transition-metal atoms and the second set is for second- and third-row atoms. For individual calculations the results could be improved by a set of parameters derived for the specific metal, but in this initial study it is important to minimize the number of variables. The necessary values for r_p are calculated as discussed above.

Table II. Parameters for Force Field Calculations

K_s cluster–C	3.0 mdyn/Å
K_s C–O	12.0 mdyn/Å
r_0 C–O	1.15 Å
$K\theta$ cluster–C–O	0.05 mdyn/radian
ϵ, vdW[a]	0.044 kcal/mol
r_0, vdW[a]	
C–C	3.8 Å
C–O	3.5 Å
O–O	3.4 Å
partial charges	C + 0.1; O −0.1
dielectric	2.5 D

	1st-row metals	2nd- and 3rd-row metals
r_t, Å	1.75	1.92
r_b, Å	2.00	2.12
r_m, Å	1.30	1.425

[a] vdW = van der Waals.

The partial charges on the carbonyl ligands are important parameters. There is a very wide range of quoted values in the literature and it seems to be a difficult value to abstract from either experiments or ab initio calculations. Considerable time was spent trying various values for the charges and it was found that the magnitude of the charge had a large effect on the magnitudes of the calculated energies but relatively little effect on the calculated geometries. Karplus has recently reported similar findings in a study of the effects of charge on calculated energies and structures of various biomolecular systems.[22] The final charge value chosen for a carbonyl ligand was set at −0.1 for the oxygen and +0.1 for the carbon atom with a neutral metal atom.

The computer program for the energy minimization was a rather unsophisticated one using a combination of direct search and Newton–Raphson minimizations based on numerical first and second derivatives. Most of the structures are the results of a full-energy minimization, but a few structures of interest do not correspond to an energy minimum. For such molecules certain bond angles were fixed or symmetry was arbitrarily imposed upon the molecule.

The Goals of the Calculations. The goals of these ligand structure calculations are rather modest when compared to the extremely precise molecular mechanics calculations now possible for most organic molecules. I am interested in learning more about the details of ligand structures, but I do not pretend to believe that experimental accuracy can even be approached. For one thing there is no way that an accurate parameterization can be made. The parameters in MM2 are based upon the experimental data from hundreds of different organic compounds. In contrast a given transition metal may only form one or two binary carbonyl compounds and they may show very different bonding modes. All metal atoms are being treated the same with no special account being given to the valence or electronic properties of individual metal atoms. The best one can hope for is a qualitative model of the steric forces that will help one to evaluate the general problem.

Precise comparisons with experimental data are also difficult due to the quoted errors in the experimental results. It is not uncommon for the uncertainty in a M–C or C–O bond length to be several hundredths of an angstrom, and bond angle errors of several degrees are not uncommon. The errors reported in most crystallographic studies are also more indicative of experimental precesion and not of accuracy since carbonyl distances and angles are only rarely corrected for an often substantial thermal motion.

The real goal of these calculations is thus not the reproduction of experimental results but the development of a model that will increase our understanding of the steric forces that determine ligand structure. Once something useful has been learned, then perhaps meaningful predictions will be possible.

Energies. The energies reported for each structure are the sums of five terms summed over all the carbonyl ligands, a cluster–carbon stretch, a carbon–oxygen stretch, a carbonyl bend, a van der Waals term, and an electrostatics term. The hypothetical zero in energy would correspond to a structure with each carbonyl

---

[22] Pettit, B. M.; Karplus, M. *J. Am. Chem. Soc.* **1985**, *107*, 1166.

Table III. Summary of Geometric and Energy Results for $M(CO)_n$ Compounds (Distances in Å, Angles in deg, Energies in kcal mol^{-1}, Steric Energy in kcal mol^{-1} CO^{-1})

cluster	point group	name	geometry	energy	steric energy
$M(CO)_4$	T_d	tetrahedron	M–C 1.76	2.67	0.67
	D_{4h}	square plane	M–C 1.78	8.70	2.17
$M(CO)_5$	D_{3h}	trigonal bipyramid	M–C 1.78 equatorial M–C 1.79 axial	13.28	2.66
	C_{4v}	square pyramid	M–C 1.79 equatorial M–C 1.78 axial ax–M–eq 100.4	13.51	2.70
$M(CO)_6$	O_h	octahedron	M–C 1.80	24.34	4.05
	D_{3h}	trigonal prism	M–C 1.82 C–M–C 83.7 within $M(CO)_3$ unit C–M–C 79.4 between $M(CO)_3$ units	35.2	5.87
$M(CO)_7$	C_{2v}	capped trigonal prism	M–C 1.88 top one M–C 1.85 middle four M–C 1.89 bottom two C–M–C 79.4 top to middle C–M–C 81.6, 94.4 middle to middle C–M–C 72.7 bottom to bottom	60.51	8.64
	C_{3v}	capped octahedron	M–C 1.89 top one M–C 1.85 middle three M–C 1.86 bottom three C–M–C 74.4 top to middle C–M–C 130.4 top to bottom	60.56	8.65
	D_{5h}	pentagonal bipyramid	M–C 1.80 axial M–C 1.89 equatorial	60.56	8.65

bound to the cluster with distances and angles corresponding to the minima of the defined potential wells and at an infinite distance from any neighboring carbonyl. At finite distances a second carbonyl will cause the energies to deviate from zero due to the nonbonded van der Waals interactions and electrostatic interactions. As the environment of a given carbonyl becomes more crowded these interactions will cause the calculated bond distances and angles to deviate from the unperturbed values.

The absolute energies reported depend upon the chosen parameters and have little significance outside the context of this paper. The relative ordering of energies and the geometries do have meaning and are not so parameter sensitive. An interesting comparison between different molecules can be made by calculating a carbonyl "steric energy". This number is calculated by partitioning the total energy calculated for a particular geometry by dividing the total energy by the number of carbonyls in the cluster.

$$E_{\mathrm{total}}/n_{\mathrm{CO}} = E_{\mathrm{steric}}$$

Single Metal Centers. The surface force field model was developed for cluster compounds, but for calibration purposes it is important to have a brief look at simple carbonyl structures with only one metal center. These results are very similar to those of a simple points on a sphere calculation as performed by many investigators over a period of many years.[23] The values found for $M(CO)_n$ (n = 4, 5, 6, or 7) systems are shown in Table III. The calculated geometries and the corresponding energies follow previous expectations. In the cases of four and six coordination the tetrahedral and octahedral structures are highly favored, while in five and seven coordination there is little difference between the isomers.

The metal–carbon bond distances in the higher coordination molecule systems are longer than in the lower coordination compounds due to the increased nonbonded repulsions of the neighboring carbonyls. The steric energies calculated for the carbonyls are also much larger for the seven-coordinate compounds than for the less crowded compounds. This relationship between carbonyl steric energy and coordination number is also found in the cluster compounds to be discussed below.

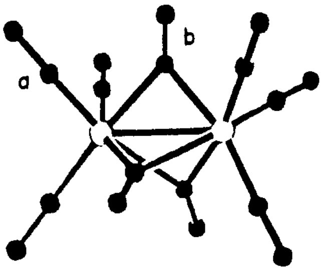

Figure 3. The minimized structure for $Fe_2(CO)_9$. The molecule has a D_{3d} geometry with structural details listed in Table V.

$Fe_2(CO)_9$. The first cluster example is $Fe_2(CO)_9$, a simple case where there is no ambiguity involving multiple isomers. The molecule has a D_{3h} geometry with three bridging CO ligands (Figure 3). The Fe–Fe bond is rather short at 2.523 Å as is common for bridged metal–metal bonds.[24] To perform the geometry calculation the metal core was given the experimentally determined geometry and the carbonyl ligands were given arbitrary initial values. The minimization routine will only converge to a local minimum so the final minimized geometry does depend upon the overall geometry selected initially. The final bond distances and angles for $Fe_2(CO)_9$ are given in Table V along with the experimental values from the Cotton and Troup structural study.[24]

The overall geometry calculated by using the surface force field is in general agreement with the experimental structure. The difference in terminal carbonyl bond distances is due to the original choice of r_t and could by improved by selecting a larger value for r_t, but to minimize variables and to allow more meaningful comparisons between different compounds the same set of distance parameters was used for all first-row transition metals. The calculated angles are the most important result in any case and they are in good agreement with the experimental results. The calculated steric energy for carbonyls of $Fe_2(CO)_9$ is 2.66 kcal,

---

(23) There are many investigations of this type: see, for example: Thompson, H. B.; Bartell, L. S. *Inorg. Chem.* **1968**, *7*, 488.

(24) Cotton, F. A.; Troup, J. M. *J. Chem. Soc., Dalton Trans.* **1974**, 800.

Table IV. Total Energies (kcal mol^{-1}) and Steric Energies (kcal mol^{-1} CO^{-1}) from Carbonyl Cluster Minimizations

cluster	point group	geometry	total energy	steric energy
$Co_2(CO)_8$	C_{2v}	M-M 2.522 Å	13.8	1.72
	D_{3d}	M-M 2.650 Å all terminal carbonyls	11.1	1.39
	D_{2d}	M-M 2.650 Å all terminal carbonyls	9.94	1.24
$Fe_2(CO)_8^{2-}$	D_{3d}	M-M 2.787 Å all terminal carbonyls	9.80	1.22
$CoFe(CO)_8^-$	C_s	M-M 2.585 one semibridging carbonyl	11.3	1.41
$Fe_2(CO)_9$	D_{3h}	M-M 2.523 Å three bridging carbonyls	24.0	2.66
$Fe_3(CO)_{12}$	C_{2v}	M-M 2 at 2.680, 2.558 Å two bridging carbonyls	28.4	2.37
	D_{3h}	M-M 2.680 Å all terminal carbonyls	33.0	2.75
	D_3	M-M 2.680 Å all terminal carbonyls	27.9	2.32
$Ru_3(CO)_{12}$	C_{2v}	M-M 2 at 2.854, 2.720 Å two bridging carbonyls	9.6	0.80
	D_{3h}	M-M 2.854 Å all terminal carbonyls	11.7	0.98
	D_3	M-M 2.854 Å all terminal carbonyls	8.7	0.72
$Co_4(CO)_{12}$	C_{3v}	M-M 3 at 2.50, 3 at 2.48 Å three bridging carbonyls	12.75	1.06
	T_d	M-M 2.50 Å all terminal carbonyls	13.6	1.13
	T	M-M 2.50 Å all terminal carbonyls	10.3	0.85
$Ir_4(CO)_{12}$	C_{3v}	M-M 2.693 Å three bridging carbonyls	2.89	0.24
	T_d	M-M 2.693 Å all terminal carbonyls	2.45	0.20
	T	M-M 2.69 Å all terminal carbonyls	0.77	0.06
$Fe_4(CO)_{13}^{2-}$	C_3	M-M 3 at 2.545, 3 at 2.610 Å one triple bridging carbonyl	22.0	1.69
$CoFe_3(CO)_{13}^-$	C_3	M-M 3 at 2.487 3 at 2.667 Å 3 asymmetric bridging carbonyls	23.1	1.78
$CrFe_3(CO)_{14}^{2-}$	D_{2d}	M-M 2.644 Å two edge-bridging carbonyls	33.1	2.36
$Mn_4(CO)_{16}$	T_d	M-M 2.644 Å 4 face-bridging carbonyls	65.2	4.66

Table IV. This is about the same as the value found for a $M(CO)_5$ compound and means that the steric energies in $Fe(CO)_5$ and $Fe_2(CO)_9$ are similar.

$M_2(CO)_8$. These compounds are both more interesting and more complicated, Figure 4. The $Co_2(CO)_8$ molecule has a fluctional structure with three isomers coexisting in solution.[6-9] One of them corresponds to the solid-state structure and has two bridging carbonyls.[5] One prominent solution isomer is though to have D_{3d} symmetry and a geometry similar to the solid-state structure of $Fe_2(CO)_8^{2-}$. The third isomer is less well characterized, but most likely it has a D_{2d} structure. Geometries have been calculated for each of these isomers with use of the surface force field. For the bridged isomer, the experimental Co–Co, 2.522 Å, bond length[4] was assumed, but the corresponding values for the nonbridged isomers are not known. Since the bond is not bridged a longer value would be expected. We recently determined the structure of the triethylphosphine monosubstituted derivative of $Co_2(CO)_8$[25] and found a nonbridged, "D_{3d}", structure with a Co–Co bond distance of 2.68 Å or 0.16 Å longer than the bridged bond in $Co_2(CO)_8$. While some of the difference may be due to the phosphine it is similar to the difference found within $Fe_3(CO)_{12}$, where the nonbridged bonds, 2.680 Å, are 0.12 Å longer than the doubly bridged bond, 2.558 Å.[26] A compromise value of 2.65 Å for the Co–Co distance in a nonbridged, $Co_2(CO)_8$ structure has thus been used for the calculation.

The experimental geometry of $Co_2(CO)_8$ is not actually C_{2v}.[4] In the solid state the structure is twisted so the Co-Co-C nonbridged angles are all different, but the deviations of up to 5° seem to be due to packing effects. The calculated geometry has a

---

(25) To be published, S. Sherlock and J. W. Lauher.

(26) Cotton, F. A.; Troup, J. M. *J. Am. Chem. Soc.* **1974**, *96*, 4155.

Table V. Selected Bond Distances (Å) and Bond Angles (deg) in $Fe_2(CO)_9$

	calcd	exptl[a]		calcd	exptl[a]
Fe–Fe	(2.523)[b]	2.523 (1)[c]	Fe–Fe–Ca	121.8	120.9 (1)
Fe–Ca	1.78	1.835 (3)	Fe–Fe–Cb	51.1	51.2 (1)
Fe–Cb	2.01	2.013 (3)	Ca–Fe–Cb′	173.0	177.1 (3)
Fe–Cb–Fe′	77.8	77.6 (1)	Ca–Fe–Cb	84.7	84.9 (3)

[a] Reference 24. [b] Calculated values in parentheses in this and subsequent tables are assumed values. [c] Errors quoted for experimental values in this and subsequent tables are taken from the original references.

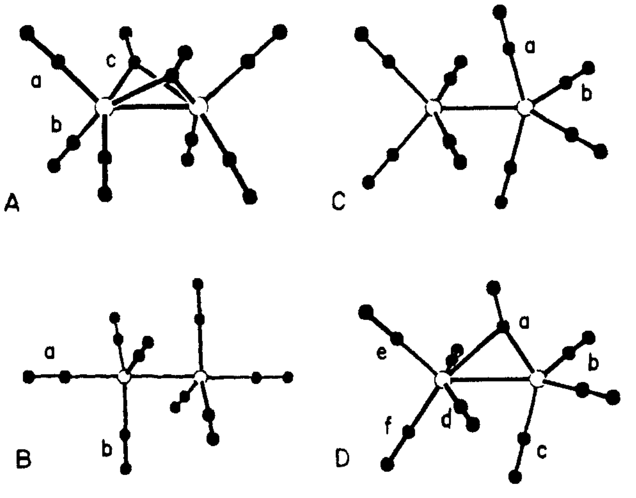

Figure 4. The minimized structures for $M_2(CO)_8$ clusters with structural details listed in Table VI: (A) C_{2v} $Co_2(CO)_8$; (B) D_{3d} $Fe_2(CO)_8^{2-}$; (C) D_{2d} $Co_2(CO)_8$; (D) C_s $CoFe(CO)_8^-$.

Table VI. Selected Calculated and Experimental Bond Distances (Å) and Bond Angles (deg) in $M_2(CO)_8$ Compounds

	calcd	exptl
	$Co_2(CO)_8$ C_{2v}	
Co–Co	(2.522)	2.522 (2)[b]
Co–Ca	1.77	1.78 (2)
Co–Cb	1.78	1.80 (2)
Co–Cc	2.01	1.92 (2)
Co–Co–Ca	138.1	123.5 (10)
Co–Co–Cb	103.8	113 (1)
Co–Co–Cc	51.2	48.5 (10)
Co–Cc–Co′	77.7	83 (10)
	$Co_2(CO)_8$ D_{3d}	
Co–Co	(2.65)	
Co–Ca	1.78	
Co–Cb	1.77	
Co–Co–Cb	84.4	
	$Fe_2(CO)_8^{-2}$ D_{3d}	
Fe–Ca	1.78	1.743 (16)
Fe–Cb	1.77	1.769 (17)
Fe–Fe–Cb	83.0	83.3 (5)
	$Co_2(CO)_8$ D_{2d}	
Co–Co	(2.65)	
Co–Ca	1.77	
Co–Cb	1.77	
Co–Co–Ca	74.0	
Co–Co–Cb	127.3	
Ca–Co–Ca	148.0	
Cb–Co–Cb	105.3	
Ca–C–Cb	99.6	
	$FeCo(CO)_8^{-1}$ C_s	
Fe–Co	(2.585)	2.585 (3)[c]
Co–Ca	1.85	1.774 (20)
Fe–Ca	2.22	2.210 (19)
Fe–C (av d–f)	1.77	1.687 (9)
Co–C (av b, c)	1.77	1.744 (20)
Fe–Co–Ca	(57.4)	57.4 (6)
Co–Fe–Ca	44.5	42.5 (5)
Co–Ca–O	154.0	151.2
Ca–Co–Cb	101.4	103.8 (20)[a]
Ca–Co–Cc	137.3	136.4 (9)
Cb–Co–Cb	106.6	110.3 (9)
Cb–Co–Cc	103.6	103.2 (9)[a]
Cd–Fe–Cd	154.5	164.1 (9)
Cd–Fe–Ce	101.2	97 (2)[a]
Cd–Fe–Cf	93.7	91.3 (20)[a]
Ce–Fe–Cf	101.1	109.2 (10)

[a] Average values. [b] Reference 4. [c] Reference 5.

rigorous C_{2v} geometry and is in general agreement but does show an informative variation from the experimental structure. The top angle Co–Co–Ca has a value of 124° less than the calculated angle of 138°. The experimental Co–Co–Cb angles average 113° and are larger than the calculate value of 103°. The net difference between the calculated and experimental geometry is an "opening up" of the metal-metal bond on the bottom of the molecule caused by an upward bending of the $M(CO)_3$ units. This may be due to a stereochemical activity of the electrons of the metal-metal bond and is in keeping with the traditional bonding picture of $Co_2(CO)_8$.

The D_{3d} isomer has one important variable, the M–M–C angle between the metal atoms and the equatorial carbonyls. In the $Fe_2(CO)_8^{2-}$ structure (Table VI) the Fe–Fe bond distance is 2.787 Å and this angle has a value of 83.3°.[5] The force field calculation gives a similar value of 83.0° and suggests that interligand repulsions are indeed the important variable in this case. For D_{3d} $Co_2(CO)_8$ a distance of 2.65 Å was assumed for the metal-metal bond and the result was a slightly larger angular value of 84.4°.

The calculated geometry for the D_{2d} isomer is shown in Figure 4c. It can be considered to be either two intertwined tetrahedra with an added metal-metal bond or as two trigonal bipyramids sharing an equatorial position as hypothesized by Lichtenberger and Brown. This configuration of ligands has the lowest energy of any we have found for the $M_2(CO)_8$ system and appears to be the global minimum for the force field. The energies of the three isomers are ordered $D_{2d} < D_{3d} < C_{2v}$, but the differences are less than 3 kcal.

The D_{2d} isomer is closely related to the structure of the $FeCo(CO)_8^-$ anion as determined by Bau.[5] In that structure one of the CO ligands on the Co atom bends over to occupy a semibridging position. The $FeCo(CO)_8^-$ structure does not correspond to a minimum in the force field calculations so it cannot be modeled in the conventional manner. To force the calculation into such a minimum a calculation was performed in which the Fe–Co–C angle of the semibridging carbon atom was fixed in addition to the positions of the two metal atoms. The metal-carbon bond distance, the oxygen of the carbonyl, and the remaining carbonyls were allowed to vary in the conventional way. The results are shown in Table VI and are in good agreement with the experimental values. The bend in the Co–C–O angle is off by only about 3° and shows the surface force field model can handle semibridging carbonyls well. The angles are reproduced better that the bond distances. The distances could be improved by changing the input values of r_t and r_b, but again this study was completed with use of only one set of distance parameters.

It is important to note that the geometry of the less symmetric $FeCo(CO)_8^-$ anion has been reproduced rather more accurately than the more symmetric $Co_2(CO)_8$ molecule. This can be interpreted as evidence that the $FeCo(CO)_8^-$ structure is governed totally by nonbonded repulsions between the carbonyl ligands, while in the $Co_2(CO)_8$ molecule the electrons of the Co–Co bond play a stereochemical role.

$M_3(CO)_{12}$. The dodecacarbonyl clusters of the iron triad show a variation with metal that has long been a subject of considerable speculation and experimental scrutiny. In the crystalline state

Table VII. Selected Calculated and Experimental Bond Distances (Å) and Bond Angles (deg) in $M_3(CO)_{12}$ Compounds

C_{2v}

	Fe calcd	Fe exptl[a,b]	Ru calcd
M–M	(2.680, 2.558)	2.680, 2.558	(2.85, 2.72)
M–Cc	1.99	2.05 (5)	2.10
M–C (av a, b, d, e)	1.78	1.82 (2)	1.93
Ca–M–Ca	171.5	172.0 (12)	172.8
Cb–M–Cb	105.0	103 (2)	106.4
Ca–M–Cb	92.6	94 (2)	92.2
Cc–M–Cc	90.0	94 (2)	88.7
Cc–M–Cd	89.3	86 (2)	89.9
Cc–M–Cd′	175.2	176 (2)	173.7
Cc–M–Ce	89.7	90 (2)	90.8
Cd–M–Cd′	91.0	95.7 (9)	90.9

D_{3h}

	Fe calcd	Ru calcd	Ru exptl[a,c]
M–M	(2.68)	(2.854)	2.854 (2)
M–Ca	1.78	1.93	1.942 (4)
M–Cb	1.78	1.93	1.921 (5)
M–M–Ca	95.5	95.8	89.5 (3)
M–M–Cb	95.5	95.1	90.3 (3)
Ca–M–Ca′	178.0	176.0	178.3 (3)
Cb–M–Cb′	109.0	109.8	104.1 (3)
Ca–M–Cb	89.4	88.8	90.3 (3)

D_3

	Fe calcd	Ru calcd
M–M	(2.680)	(2.854)
M–Ca	1.78	1.93
M–Cb	1.78	1.93
M–M–Ca	76.1, 99.3	73.5, 99.5
M–M–Cb	100.1, 153.3	102.2, 154.3
Ca–M–Ca′	174.8	172.1
Cb–M–Cb′	104.1	100.1
Ca–M–Cb	91.1, 92.1,	91.7, 93.3

[a] Average values. [b] Reference 26. [c] Reference 27.

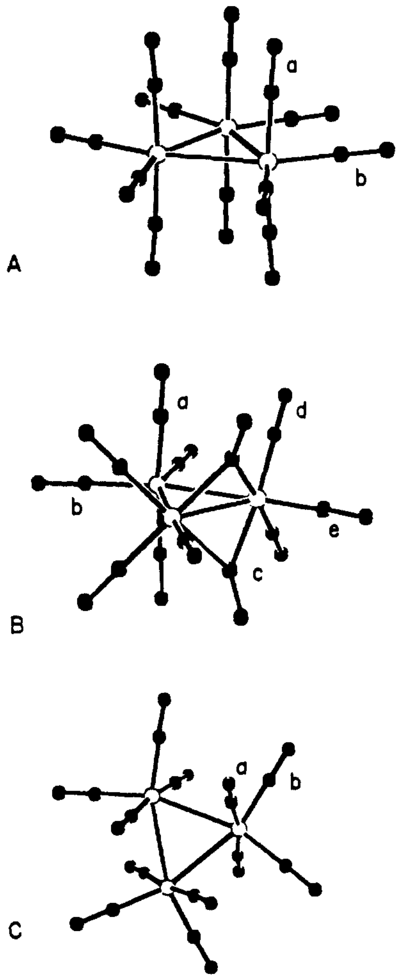

Figure 5. The minimized structures for $M_3(CO)_{12}$ clusters with structural details listed in Table VII: (A) D_{3h}; (B) C_{2v}; (C) D_3.

the iron compound, $Fe_3(CO)_{12}$, has an approximate C_{2v} symmetry with two carbonyls bridging one metal–metal bond.[26] The ruthenium and osmium analogues have all terminal structures with D_{3h} symmetries.[27,28] Various phosphine or phosphite derivatives of $Ru_3(CO)_{12}$ have been shown to have a D_3 structure that is related to the D_{3h} terminal structure by a concerted rotation or twisting of the $M(CO)_4$ groups.[29] One tetraphosphine-substituted ruthenium cluster has a bridged structure similar to the C_{2v} geometry of the iron compound.[30] With use of the surface force field two sets of minima have been calculated for each of these isomers by using first the standard distance parameters used for first-row transition metals and second a second set of distance parameters representative of second- and third-row metals. The principal structural features resulting from these calculations are outlined in Table VII and illustrated in Figure 5.

The model iron and ruthenium structures are very similar; the ruthenium structures have longer bond distances, but the angular arrangements of the carbonyls are nearly the same. This illustrates the point made early that the actual calculated geometries are not very parameter sensitive. The energies calculated for the iron isomers are much higher than those calculated for the analogous ruthenium compounds. This is due to the fact that the carbonyls are more closely packed in the iron compound.

The calculated C_{2v} structure for $Fe_3(CO)_{12}$ agrees reasonable well with the experimental structure but has exact C_{2v} symmetry. The actual crystal structure shows a more asymmetric structure with a pair of compensating semibridging carbonyls.[26] This asymmetry amounts to about a 0.2-Å difference in the iron–carbon bond distances and can be modeled by restraining the Fe–Fe–C angles to defined values in the same manner that the $FeCo(CO)_8^-$ ion was handled above. Calculations done with such an asymmetric restraint show only a minor variation in the calculated energy and little change in the other structural parameters.

The calculated D_{3h} structure for $Ru_3(CO)_{12}$ again has ideal symmetry, while the crystal structure shows angular deviations of about 4° from an ideal D_{3h} geometry. Of particular interest are the M–C–O angles about the axial carbon atoms. In the crystal structure the axial carbonyls are bent outward by an average of 7° while the equatorial carbonyls show little deviation from 180°. In the calculated structure the axial carbonyls bend out 4°, while the equatorial carbonyls remain linear. The amount of axial bend in the calculated geometries does depend upon the magnitude of K_θ, the angular force constant, but this value is already set to a relative low value and decreasing it further does not seem appropriate.

The D_3 structure is not known for any binary carbonyl but is found in phosphine- and phosphite-substituted iron and ruthenium carbonyls. It is formed by twisting the $M(CO)_4$ units of the D_{3h} isomer. The D_{3h} isomer has significant axial–axial and equatorial–equatorial interactions that are relieved by this twisting. The axial carbonyls are carried by the twist into positions approaching semibridging; the Ru–Ru–C bond angle is calculated to be 73.5°. In some of the actual experimental structures semibridges do form. For example, in the mixed-metal compound, $FeRu_2(CO)_{10}\{PPh_3\}_2$, the two axial carbonyls on the iron atom are semibridging with Ru–Fe–C angles of 64°.[29] Johnson has hypothesized that the D_3 isomer may be the favored isomer of $Fe_3(CO)_{12}$ in solution.[11] These calculations would support that idea.

The absolute energies calculated for these various isomers have little meaning, but it is quite instructive to compare the relative

---

(27) Churchill, M. R.; Hollander, F. J.; Hutchinson, J. P. *Inorg. Chem.* **1977**, *16*, 2655.

(28) Churchill. M. R.; DeBoer, B. G. *Inorg. Chem.* **1977**, *16*, 878.

(29) Venalainen, T.; Pakkannen, T. *J. Organomet. Chem.* **1984**, *266*, 269.

(30) Bruce, M. I.; Matison, J. G.; Patrick, J. M.; White, A. H.; Willis, A. C. *J. Chem. Soc., Dalton Trans.* **1985**, 1223.

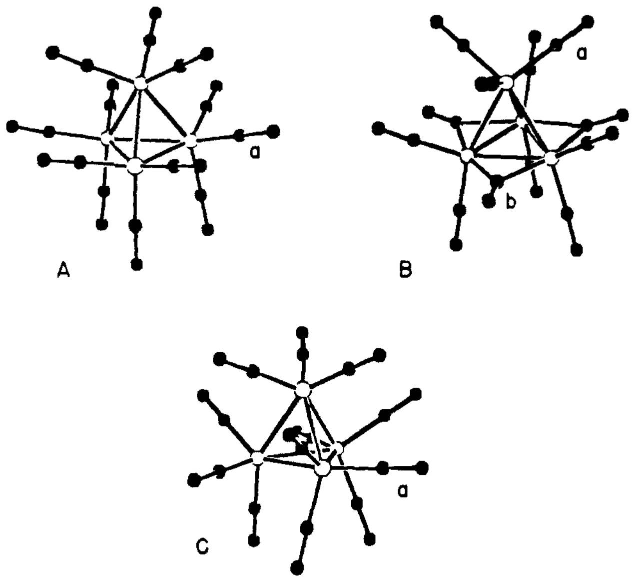

Figure 6. The minimized structures for $M_4(CO)_{12}$ clusters with structural details listed in Table VIII: (A) T_d, (B) C_{3v}; (C) T.

energies calculated for the iron and ruthenium cases. The D_3 and C_{2v} isomers both have a pseudoicosahedral ligand packing and are lowest in energy for both iron and ruthenium. The D_{3h} isomer has an anticubeoctahedral packing of the carbonyls and is the least stable in each case. However, the smaller iron cluster requires a tighter carbonyl packing and thus shows larger differences in energy. The D_{3h} isomer is 2.1 kcal less stable than bridged isomer in $Ru_3(CO)_{12}$ but 4.6 kcal less stable in $Fe_3(CO)_{12}$.

The facts show that the Ru compound actually adopts the geometry of the sterically less favored isomer, while the iron compound does not. This can be explained by invoking a metal-based valence or electronic factor that favors the D_{3h} structure. A simple hybridization argument may be sufficient; in the D_{3h} isomer each metal atom has a pseudooctahedral coordination and is presumably well set up for the formation of six strong bonds. In the D_3 and C_{2v} isomers the coordination geometry about each metal is not so regular. This argument can also be stated with use of Hoffmann's fragment molecular orbital approach. A $M(CO)_4$ fragment has two frontier orbitals and is isolobal to a methylene group. Three such groups would prefer to bond with a strict D_{3h} symmetry. Twisting the groups into sterically more favorable geometries destroys the favorable overlap. In $Fe_3(CO)_{12}$ it would appear that the steric constraints due to carbonyl crowding dominate, while in $Ru_3(CO)_{12}$ the orbital constraints seem to be more important.

$M_4(CO)_{12}$. The tetranuclear dodecacarbonyl metal clusters of the cobalt triad are relatively strain free molecules when compared to the trinuclear dodecacarbonyls, Figure 6. This is a simple function of the change in coordination number from a average of four in $M_3(CO)_{12}$ clusters to an average of three in $M_4(CO)_{12}$ clusters. The two isomers observed experimentally for the $M_4(CO)_{12}$ clusters are the C_{3v}-bridged structure found[31,32] for $Co_4(CO)_{12}$ and $Rh_4(CO)_{12}$ and the approximate T_d all-terminal structure found for $Ir_4(CO)_{12}$.[33] Presumably the Ir structure differs from the Rh structure for valence or electronic reasons since with similar metallic radii the steric factors in Rh and Ir compounds should be essentially the same. Calculated geometries for the C_{3v} and T_d isomers are compared with the experimental values for $Co_4(CO)_{12}$ and $Ir_4(CO)_{12}$ in Table VIII. The crystal structures of both compounds are highly disordered and were very difficult experimental problems, thus the quoted experimental values have large errors.

Table VIII. Selected Calculated and Experimental Bond Distances (Å) and Bond Angles (deg) in $M_4(CO)_{12}$ Compounds

C_{3v}

	Co calcd	Co exptl[a,b]	Ir calcd
M-M	(2.500, 2.480)	2.50, 2.48	(2.693)
M-C (av term)	1.77	1.83 (2)	1.93
M-Cb	1.99	2.04 (2)	2.10
M-Cb-M	77.3	75 (1)	79.6
M-Cb-O	141.4	142 (1)	140.2
M′-M-Ca	96.7	97 (1)	99.4

T_d

	Co calcd	Ir calcd	Ir exptl[a,c]
M-M	(2.50)	(2.693)	2.693 (5)
M-Ca	1.77	1.93	
M′-M-Ca	97.2	96.8	97 (2)
Ca-M-Ca′	100.0	100.6	99 (2)

T

	Co calcd	Ir calcd
M-M	(2.50)	(2.693)
M-Ca	1.76	1.92
M′-M-Ca	86.7	86.7
Ca-M-Ca′	100.0	103.3

[a] Average values. [b] Reference 31. [c] Reference 33.

The global minimum in the $M_4(CO)_{12}$ system appears to correspond to a third isomer that has not been observed experimentally. This isomer has T symmetry and is analogous to the D_3 isomer in the $M_3(CO)_{12}$ system. The T isomer can be constructed by taking the T_d isomer and by rotating or twisting in a concerted manner each $M(CO)_3$ unit about the local threefold axis. The T isomer has never been found for a $M_4(CO)_{12}$ derivative, but as shown below it does serve as the basis for the structure of $M_4(CO)_{13}$ clusters. It should be noted that the crystal structure of $Ir_4(CO)_{12}$, normally quoted as having T_d symmetry, actually shows a twisted molecule with C_3 site symmetry. The disorder in the structure made it difficult for Churchill and Hutchinson to sort out the true structure, but there is a definite twist of a few degrees in the $M(CO)_3$ groups that removes the T_d symmetry. An isolated $Ir_4(CO)_{12}$ molecule may thus indeed have T point group symmetry but with a smaller than calculated deviation from T_d.

The carbonyl packing in the calculated T isomer corresponds to a distorted icosahedron. The T point group is a subgroup of the I_h point group, and the resulting structure has twofold and threefold axes with no mirror planes. The C_{3v} bridged isomer also has a distorted icosahedral packing of the carbonyls and the C_{3v} isomer can be converted into the T isomer by a rotation of about 12° of the M_4 metal core within the carbonyl polyhedron. In the T isomer each of the 12 carbonyl ligands lies in the plane of one face of the metal tetrahedron with a M-M-C bond angle of 86.7° and with a small movement could assume a semibridging position. Carbonyl scrambling in $Co_4(CO)_{12}$ has been hypothesized to go via a T_d intermediate, but an interconversion via the T isomer would require less movement of the carbonyls and would seem to be a lower energy pathway. It should also be noted that since the T point group contains only proper rotation axes, a T isomer of a $M_4(CO)_{12}$ compound would be chiral and a twist of the $M(CO)_3$ groups in either the left- or right-hand direction will give enantiomers.

$Fe_4(CO)_{13}^{2-}$. Adding a 13th carbonyl to a tetranuclear system causes a major increase in the calculated strain energy. Two separate crystallographic studies of the $Fe_4(CO)_{13}^{2-}$ anion have been reported. Doedens and Dahl studied the $Fe(pyr)_6^{2+}$ salt and found a structure that can be described as a derivative of the C_{3v} $M_4(CO)_{12}$ structure in which a 13th carbonyl has been added to the bottom face with the metal core then rotated relative to the carbonyl polyhedron, changing the symmetrical bridging carbonyls into semibridging carbonyls.[34] Kaesz and co-workers studied the

---

(31) Carre, F. H.; Cotton, F. A.; Frenz, B. A. *Inorg. Chem.* **1976**, *15*, 380.
(32) Wei, C. H.; Wilkes, G. R.; Dahl, L. F. *J. Am. Chem. Soc.* **1967**, *89*, 4792.
(33) Churchill, M. R.; Hutchinson, J. P. *Inorg. Chem.* **1978**, *17*, 3528.
(34) Doedens, R. J.; Dahl, L. F. *J. Am. Chem. Soc.* **1966**, *88*, 4847.

Table IX. Selected Calculated and Experimental Bond Distances (Å) and Bond Angles (deg) in the $Fe_4(CO)_{13}^{2-}$ Anion

	calcd	exptl $Fe(pyr)_6^{2+}$ salt[a,b]	exptl PPN^{+1} salt[a,c]
Fe–Fe	(2.545, 2.610)	2.50 (1), 2.58 (1)	2.545 (2), 2.610 (2)
Fe–Cc	1.83	1.80 (4)	1.79 (1)
Fe′–Cc	2.25	2.28 (4)	2.67 (1)
Fe–Ce	2.07	2.00 (3)	2.05 (1)
Fe–Cc–O	158.1	155 (2)	172.1 (9)
Fe–Ce–O	134.7	134 (2)	134.1 (4)
Fe–Fe′–Ca	95.4	97 (1)	94.7 (3)
Fe′–Fe–Cb	78.4	77 (1)	75.0 (3)
Fe′–Fe–Cc	86.1	86 (1)	93.4 (3)
Fe′–Fe–Cd	168.8	171 (2)	164.1 (3)

[a] Average values. [b] Reference 34. [c] Reference 35.

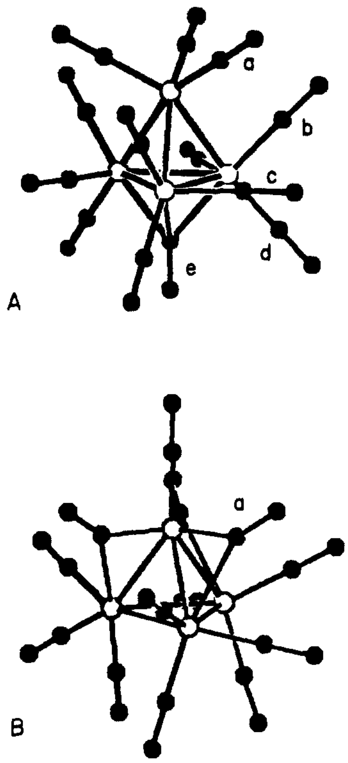

Figure 7. The minimized structures for $M_4(CO)_{13}$ clusters with structural details listed in Table IX. Notice how both structures are closely related to the T isomer of the $M_4(CO)_{12}$ series shown in Figure 6c. In A the thirteenth carbonyl adds to the base of the tetrahedron, while in B the thirteenth carbonyl adds to the apex of the tetrahedron: (A) C_3, $Fe_4(CO)_{13}^{2-}$; (B) C_3, $CoFe_3(CO)_{13}^{-}$.

PPN^+ salt and found a similar structure except the rotation of the metal core had proceeded further converting the semibridging carbonyls into essentially terminal or marginally semibridging positions.[35] This seemingly irregular structure was hypothesized to represent a structure along a valence tautomeric coordinate corresponding to the C_{3v} to T_d isomer interconversion in a $M_4(CO)_{12}$ system.[35] Actually it is much better viewed as a derivative of the missing T isomer of the $M_4(CO)_{12}$ system!

The calculated geometry for $Fe_4(CO)_{13}^{2-}$ using the surface force field is given in Table IX and is closest to the Dahl structure. As shown in Figure 7A, the terminal carbonyl ligands are arranged such that there are indeed three carbonyls approximately in each face of the M_4 tetrahedron. A very similar structure was found for the methyl derivative of this anion, $Fe_4(CO)_{12}(COMe)^-$.[36,37] In the methyl compound the T arrangement of the $M_4(CO)_{12}$ portion of the molecule is also found with one of the carbonyls belonging to the top $Fe(CO)_3$ group actually assuming a semibridging position.

Table X. Selected Calculated and Experimental Bond Distances (Å) and Bond Angles (deg) in $CoFe_3(CO)_{13}^-$ Anion

	calcd	exptl[a,b]
Co–Fe	(2.487)	2.487 (5)
Fe–Fe	(2.667)	2.667 (5)
Co–Ca	1.82	1.83 (3)
Fe–Ca	2.48	2.02 (3)
Co–Ca–O	156.6	142 (2)
Fe–Ca–O	127.7	137 (2)
Fe–Ca–Co	74.6	80 (1)

[a] Average values. [b] Reference 36.

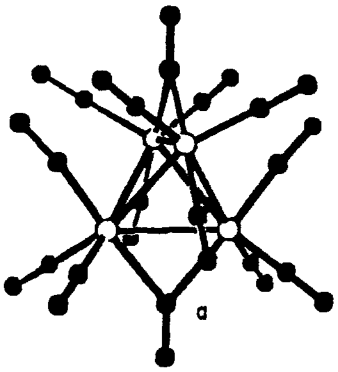

Figure 8. The minimized structure for the cluster $CrFe_3(CO)_{14}^-$ with structural details listed in Table X. In the calculation all metals were given the same parameters, thus giving the final structure a D_{2d} geometry.

$CoFe_3(CO)_{13}^-$. This cluster is isoelectronic to the $Fe_4(CO)_{13}^{2-}$, but it has a different ligand structure reflecting the asymmetry introduced by the cobalt atom.[38] The 13th carbonyl adds to the apical cobalt atom instead of the basal iron face of the cluster, Figure 7B. As shown in the crystal structure the remaining 12 carbonyls again are approximately arranged in the T geometry about the M_4 core. The three original carbonyls bound to the cobalt move down into asymmetric bridging positions to the iron atoms. A structure was calculated for this ion by using the minimized T structure for the $M_4(CO)_{12}$ system as a starting point with an additional terminal CO added to one of the metal atoms. The minimization converged to a structure very similar to the experimental structure except the asymmetric bridges showed even greater asymmetry in the calculated structure. This difference may be due to excluded valence forces, since in the anion the iron atoms are formally electron deficient and should have a somewhat greater attraction for the bridging carbonyls. In the calculation all metal atoms were identical.

$M_4(CO)_{14}$ and Beyond. Until recently according to folk lore it was though to be impossible to prepare a tetrahedral cluster with more than 13 carbonyl ligands. Horwitz, Holt, and Shriver destroyed the myth by reporting the synthesis and structural study of the compounds $MFe_3(CO)_{14}^{2-}$ (M = Cr, Mo, or W).[19] The Cr compound has a structure that can be described as a derivative of the $M_4(CO)_{12}$ T_d structure with the two extra carbonyls bridging two opposite edges of the tetrahedron of metal atoms. The actual structure is distorted from this ideal picture, because of asymmetry introduced by the Cr atom; the carbonyl that bridges a Cr–Fe bond is notably asymmetric. Horwitz et al. performed an analysis of the steric crowding within this molecule using a simplified force-field procedure and concluded that the total repulsion energy due to carbonyl packing was about 36 kcal.[19] With use of the surface force field model a geometry was calculated for an idealized $M_4(CO)_{14}$ structure (Figure 8) resulting in a total energy of 33.1 kcal. The rough agreement between the numbers

---

(35) van Buskirk, G.; Knobler, C. B.; Kaesz, H. D. *Organometallics* **1985**, *4*, 149.

(36) Holt, E. M.; Whitmire, K.; Shriver, D. F. *J. Chem. Soc., Chem. Commun.* **1980**, 778.

(37) Dawson, P. A.; Johnson, B. F. G.; Lewis, J.; Raithby, P. R. *J. Chem. Soc., Chem. Commun.* **1980**, 781.

(38) Horwitz, C. P.; Holt, E. M.; Shriver, D. F. *Organometallics* **1985**, *4*, 1117.

Table XI. Selected Calculated and Experimental Bond Distances (Å) and Bond Angles (deg) in the $CrFe_3(CO)_{14}^{2-}$ Anion

	calcd	exptl[a]
M–M	(2.644)	2.633 (25) Cr–Fe 2.655 (4) Fe–Fe
M–Ca	2.02	2.24 (2) Cr 1.95 (2), 1.99 (2), 2.04 (2) Fe
M–O (av term)	1.78	1.73 (2) Cr 1.78 (2) Fe
M–Ca–O	139.1	128.8 (14) Cr 144.4 (16), 134.7 (14), 152.1 (14) Fe

[a] Reference 19.

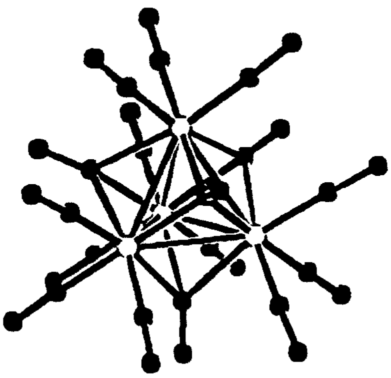

Figure 9. The minimized structure for the hypothetical cluster compound $Mn_4(CO)_{16}$ with T_d symmetry.

is probably more coincidental than anything else, but it does indicate that the two methods are calibrated in a similar manner.

The total energy value of 33.1 kcal corresponds to a steric energy of 2.35 kcal per CO. This is similar to the value of 2.37 kcal calculated for $Fe_3(CO)_{12}$ and suggests that the steric crowding in $CrFe_3(CO)_{14}^{2-}$ is similar to that in $Fe_3(CO)_{12}$. It was noted that the bond distances in $CrFe_3(CO)_{14}^{-}$ are longer than normal, averaging 2.64 Å, presumably due to the steric crowding. The nonbridged bonds of $Fe_3(CO)_{12}$ are actually longer, 2.68 Å, also indicating a high degree of steric crowding.

Finally it is interesting to ask if a tetrahedral cluster with more that 14 carbonyls would be possible. A minimized geometry, Figure 9, was calculated for a hypothetical 60-electron compound, $Mn_4(CO)_{16}$, using the geometry of $Re_4(CO)_{12}H_4^{4-}$ as a model.[39] The Re anion has T_d symmetry with the 12 terminal carbonyls eclipsed and the hydrogen atoms bridging the four faces of the tetrahedron. A $Mn_4(CO)_{16}$ compound with such a geometry has a total energy of 65 kcal when the standard first-row transition-metal parameters and a metal–metal bond distance of 2.64 Å are used. This corresponds to a steric energy of 4.1 kcal per CO, about the same as the value found for octahedral $M(CO)_6$. With a larger second- or third-row metal the energy will of course be considerably smaller. Thus there appears to be no steric problem preventing the existence of a compound such as $Re_4(CO)_{16}$, although there may be serious problems with its electronic structure.[40]

Conclusions. The goal of this work was the developement of a surface force field model for the simulation of ligand structures in transition-metal carbonyl clusters. The outlined model does indeed reproduce the general features of such compounds rather well, perhaps better than one might have expected considering the arbitrary nature of the parameters. With improved parameters for the specific metal being modeled even better agreement may be expected.

The calculated steric energies are quite interesting. Not surprisingly the highest energies are found for the clusters with the highest carbonyl to metal ratios, $Fe_2(CO)_9$, $Fe_3(CO)_{12}$, and $CrFe_3(CO)_{14}^{-}$. The M_2 clusters seem to be special, but in general there is a relation between high steric energy and long metal–metal bonds. The high-energy $Fe_3(CO)_{12}$ and $CrFe_3(CO)_{14}^{-}$ species have the longest metal–metal bonds of all the first-row clusters studied. On the other hand, $Co_4(CO)_{12}$ has the shortest metal–metal bonds and the lowest calculated steric energies.

The second- and third-row transition metals have larger radii and thus lower carbonyl steric energies. $Ru_3(CO)_{12}$ and $Ir_4(CO)_{12}$ appear to have very little steric interaction of any kind between carbonyl ligands. Thus it is not surprising that they adopt structures that are electronically favorable but sterically the least favorable.

Extensions of the Model. The model has no size limitations and clusters of any size, including bulk metal surfaces, can be treated by using the existing methods. However, with a large number of carbonyl ligands there can be a large number of local minima and the starting geometries must be chosen with more care.

For the calculations in this paper a rigid metal core was assumed. Not all metal geometries will have an identical energy and some force constant should be assigned for metal–metal stretches. The parameters to be chosen are not obvious, however, and will likely be different for each cluster geometry and for each element.

The force-field procedures give no accounting to the electronic or valence forces associated with a compound. Experimental structures generally correspond well to one of the local minima in the force field, but the particular minimum is often not the global minimum. Thus the use of the surface force-field method in conjuntion with one of the standard molecular orbital programs should be of great value.

Extensions to other ligand systems are the next goal. The parameters for most organic ligands can be taken directly from the established MM2 list with the addition of suitable values for cluster–ligand stretches, but the computer programming is quite complex. The ligand structures of hydrido carbonyl clusters and of mixed cyclopentadienyl carbonyl clusters are present under investigation.

Acknowledgment. This work was generously supported by a grant from the National Science Foundation. The calculations were performed on the departmental VAX 11/780 computer that was acquired with funds provided by the NSF and the State University of New York. Special thanks go to my many friends at the Brook with whom many hours have been devoted to discussions of this work.

---

(39) Saillant, R.; Barcelo, G.; Kaesz, H. *J. Am. Chem. Soc.* **1970**, *92*, 5739.

(40) Hoffmann, R.; Schilling, B. E. R.; Bau, R.; Kaesz, H. D.; Mingos, D. M. P. *J. Am. Chem. Soc.* **1978**, *100*, 6088.